

Disorder and surface effects on work function of Ni-Pt metal gates

Guigui Xu, Qingyun Wu, Zhigao Chen, and Zhigao Huang*

Department of Physics, Fujian Normal University, Fuzhou 350007, People's Republic of China

Rongqin Wu and Yuan Ping Feng†

Department of Physics, National University of Singapore, 2 Science Drive 3, Singapore 117542, Singapore

(Received 22 May 2008; published 19 September 2008)

Work functions of NiPt alloys with different compositions are investigated using first-principles methods based on density-functional theory. Results of our calculations reveal that surface alloy composition has a significant effect on the work function of the NiPt alloy. However, for a given surface composition, the work function is insensitive to the distributions of Ni/Pt atoms in the alloy and it is only slightly affected by alloy disorder. Our work suggests surface atomic modification as a promising way of tuning the work function of alloy metal gate.

DOI: [10.1103/PhysRevB.78.115420](https://doi.org/10.1103/PhysRevB.78.115420)

PACS number(s): 73.30.+y, 68.35.Dv, 68.35.bd

I. INTRODUCTION

The continual downscaling of semiconductor devices is now near its limit as the gate dielectric becomes too thin to prevent a tolerable leakage current. To overcome this limit, replacement of silicon dioxide (SiO_2) gate dielectric by high dielectric constant (high- k) materials is required¹⁻³ and, at the same time, metal gates should be used instead of the polycrystalline Si (poly-Si) gate electrodes.⁴⁻⁶ Metal gates are indispensable as to avoid poly-Si depletion, poly-Si dopant penetration, and incompatibility of poly-Si with high- k dielectrics.⁷ The criteria for proper metal gates is that their work functions should be close to the conduction- and valence-band edges of silicon for n - and p -channel metal-oxide-semiconductor field-effect transistors (MOSFETs), respectively.^{8,9} There are metals with work functions meeting either but rarely both. So, many strategies have been proposed to achieve this goal. Metal nitrides and metal silicides as alternative metal gates have been intensively investigated.^{7,10-12} Their work functions, nevertheless, are close to the midgap of silicon rendering the threshold voltage too high to be useful in bulk MOSFETs. The tuning technique of the work function realized by metal stacks^{6,13} has been suggested. However, material selection and interface manipulation remain a challenge because of material compatibility with the conventional complementary metal-oxide semiconductor flow and lattice mismatch. Work-function modulation using binary alloys has been studied in experiments.^{14,15} Recently, Park *et al.*⁶ has found that submonolayer of an overlying metal can affect the work function of the NiAl and PtAl systems significantly. Up to now, however, the influence of the disorder at the surface and in the bulk on the work functions of metal alloys has not been studied.

Bulk Ni and Pt have very different work functions even though they share the same crystal structure. Moreover, NiPt is a typical example of a random alloy. Substitutional solid solution with fcc structure can be formed over the entire composition range and a wide range of temperature. Therefore, NiPt alloy may be a good candidate for tuning the metal gate work function. In this paper, we focus on the effects of disorder and surface composition on the work function of

NiPt metal alloy gates. In Sec. II, the computational details are introduced. In Sec. III A, the effect of disorder on the work function of NiPt alloys is studied. It is found that for a given surface composition disorder has a small effect on the work function. In Sec. III B, the effect of surface on the work function of NiPt alloys is investigated. It is observed that Pt doping in the surface layer not only has a significant effect on the work function but it is also energetically favored. Finally, a conclusion is given in Sec. IV.

II. METHOD

The work functions of the (001) surface of the NiPt alloy were studied using first-principles method based on the density-functional theory (DFT).¹⁶ All calculations were carried out using the Vienna *ab initio* simulation package¹⁷ with the generalized gradient approximation (GGA) (Ref. 18) and projector augmented wave potential.¹⁹ The metal surface was modeled using a slab model and periodic boundary conditions were applied with 12 Å of vacuum between the slabs. Γ -centered $3 \times 3 \times 1$, $6 \times 6 \times 1$, and $11 \times 11 \times 1$ k meshes were adopted to sample the Brillouin zone for 3×3 , 2×2 , and 1×1 supercells, respectively. A cut-off energy of 300 eV was used for the plane-wave expansion of electron wave function. These parameters ensure a convergence better than 1 meV for the total energy. The atomic coordinates in the supercell were fully relaxed using the conjugate-gradient algorithm²⁰ until the maximum force on a single atom was less than 0.05 eV/Å. After relaxation, the work functions were calculated as the differences between the electrostatic potential in the middle of the vacuum region and the metal Fermi energy.

Convergence test with respect to the number of layers was carried out with a 1×1 surface unit cell. It was found that a slab consisting of a minimum of four metal layers is required to converge the work function. Subsequent calculations of the work functions of low index (001) surface were performed using slabs of eight layers and a 3×3 surface unit cell. The calculated work function of the clean Ni (001) (5.09 eV) agrees with the experimental value⁶ and that of Pt (001) (5.85 eV) is also in good agreement with results of similar

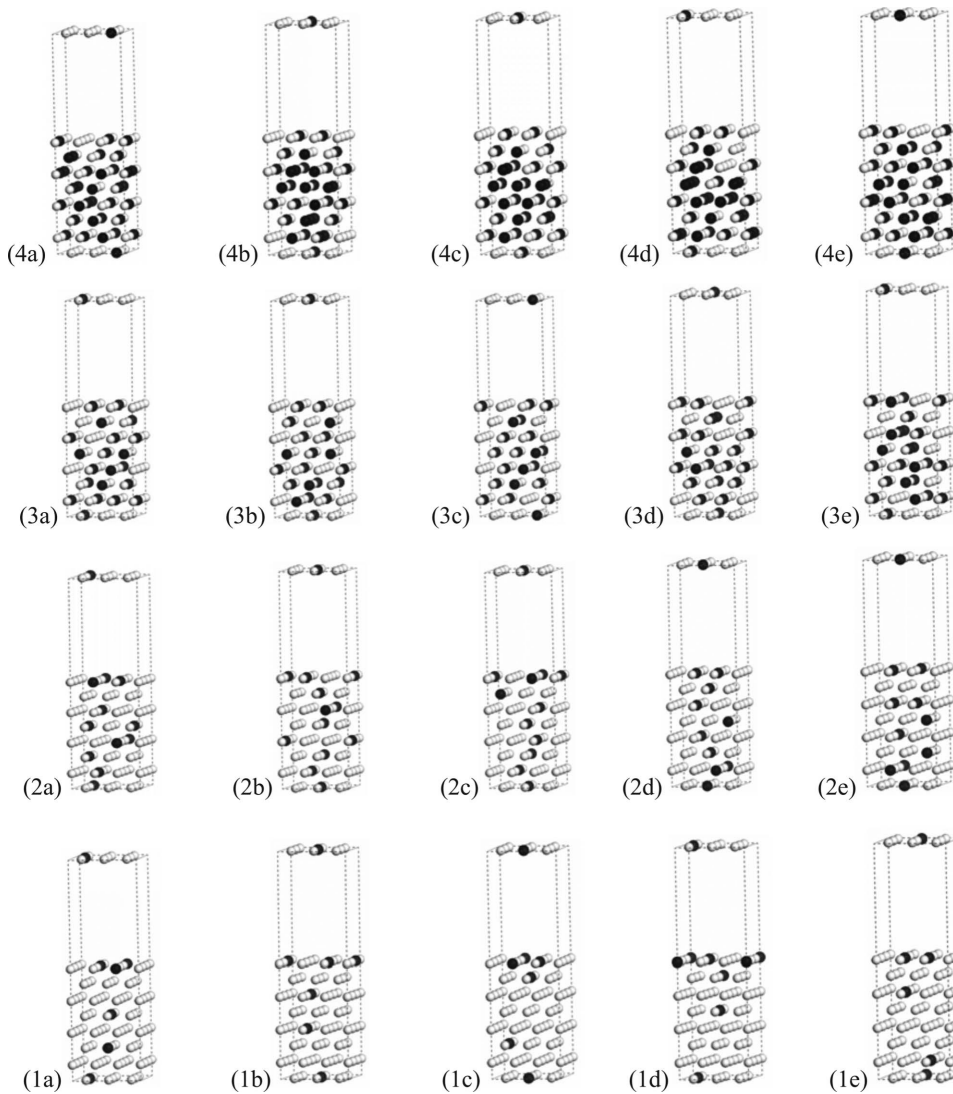


FIG. 1. Atomic models (supercells) of $\text{Ni}_{1-x}\text{Pt}_x$ (001) surfaces using eight layers of 3×3 surface unit cell. (1a–1e) $\text{Ni}_{0.935}\text{Pt}_{0.065}$, (2a–2e) $\text{Ni}_{0.875}\text{Pt}_{0.125}$, (3a–3e) $\text{Ni}_{0.75}\text{Pt}_{0.25}$, and (4a–4e) $\text{Ni}_{0.625}\text{Pt}_{0.375}$ (light: Ni; black: Pt).

calculation based on GGA,²¹ which, however, is ~ 0.3 eV smaller than the local-density approximation (LDA) value.⁶ This can be attributed to the difference between GGA and LDA methods.

III. RESULTS AND DISCUSSION

A. Effects of disorder on work function

The surface models used in our calculations are shown in Fig. 1. Using a slab of eight (001) atomic layers and 12 vacuum layers with a 3×3 surface unit cell, the supercell contains 72 atoms; nine in each layer. To investigate the composition dependence of metal work function, $\text{Ni}_{1-x}\text{Pt}_x$ alloys with four different compositions, $x=0.065$, 0.125, 0.25, 0.375, respectively, are considered in the present study. For a given composition, there exist a large number of arrangements of Ni and Pt atoms in the fcc lattice. The details of such atomic arrangements may affect the work function of the alloy. However, instead of simulating a truly random alloy, we took a simple approach and chose arbitrarily five typical disordered structures for each composition to qualitatively evaluate how much alloy disorder affects its work

function. The corresponding supercells are shown in Fig. 1. It turned out that the work function of the alloys is sensitive to the composition in the surface layer but is less sensitive to the disorder of the alloy as discussed in the following. In our study of disorder dependence of the metal work function, the numbers of Pt atoms on the top and on the bottom layers of the slab are fixed at two and one, respectively.

If the $\text{Ni}_{1-x}\text{Pt}_x$ alloy is ordered, every Ni(Pt) atom should have the same coordination structure. That is, every Ni(Pt) should have a definite number of nearest-neighbor Ni or Pt atoms. For example, for pure Pt alloy, every Pt atom has 12 nearest-neighbor Pt atoms. For the ordered $\text{Ni}_{0.75}\text{Pt}_{0.25}$ alloys, every Pt atom should have eight nearest-neighbor Ni atoms and four nearest-neighbor Pt atoms. On the contrary, for a disordered $\text{Ni}_{1-x}\text{Pt}_x$ alloy, Pt(Ni) atoms may have various coordination structures. For example, Pt atoms in the alloys in principle can have 0, 1, 2, ... or 12 nearest-neighbor Ni atoms. As a measure of randomness of the $\text{Ni}_{1-x}\text{Pt}_x$ alloy, the number of Pt atoms (n) that have the same number (m) of nearest-neighbor Ni atoms within the 72-atom supercell is counted and the results are presented in Fig. 2 for various models and alloy compositions being studied. Such an approach was used to represent the disorder/order of Si and Al

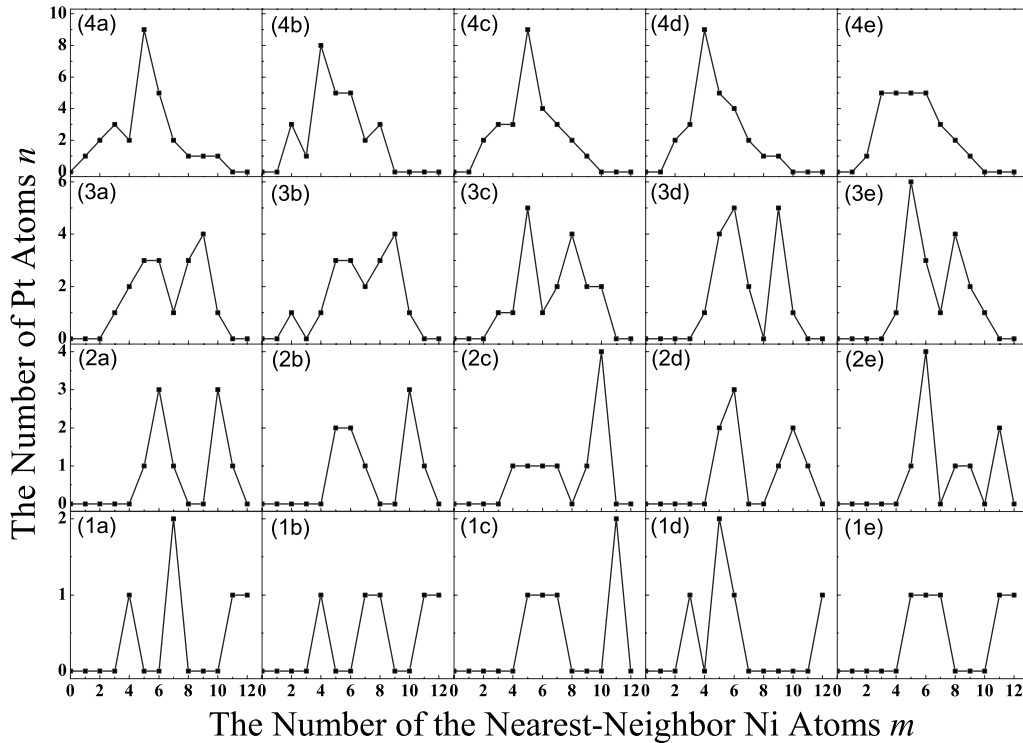


FIG. 2. The number of Pt atoms n that have m nearest-neighbor Ni atoms in various atomic models (supercells) given in Fig. 1.

in aluminosilicate faujasites.²² For example, $m=6$ and $n=5$ means that among the 72x Pt atoms (in the case of $x=0.065$, the number of Pt atoms is taken to be five) in the supercell, five of them have six nearest-neighbor Ni atoms. In the case of $x=0.125$, as shown in Fig. 2 (2a), the total number of Pt atoms is nine. The highest Ni coordination of Pt atom is 11 and only one Pt atom has that. Three of the nine Pt atoms have ten Ni nearest neighbors each. Another three Pt atoms have six Ni atoms as their nearest neighbors. The remaining two Pt atoms have five and seven Ni nearest neighbors, respectively. From the figures, it is clear that the Pt distributions in the supercell are quite complex and the five structural models for each alloy composition are fairly good representations of random alloys.

In epitaxial growth, the lattice constant is a measure of the structural compatibility between different materials. Materials, which can be lattice matched to Si-high k , are of interest

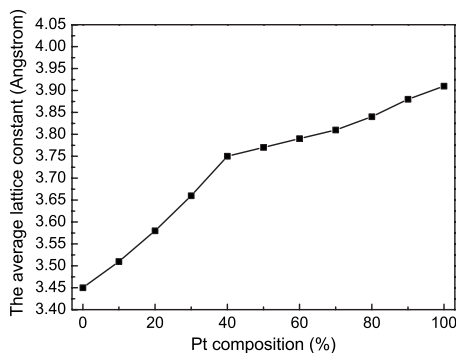


FIG. 3. Variation of the average lattice constant a with composition x .

in semiconductor technology. So it is important to investigate how the lattice constant changes with composition. In our calculations, it is found that the lattice constant is essentially independent of disorder. For example, the standard deviations of the calculated lattice constants are less than 0.006 Å for the various alloy compositions being considered. The average lattice constant a (Å) is shown as a function of Pt content x in Fig. 3. The lattice constant increases with Pt content due to the larger atomic radius of Pt relative to Ni. The rates of increase, however, is different in Ni-rich and Pt-rich alloys indicating deviation from the Vegard's law.²³ Based on the calculated lattice constant, we can obtain good lattice match to high- k gate dielectrics such as HfO_2 , ZrO_2 , and their silicates, which allows fabrication of high-quality metal-oxide interface by varying the composition of the alloy. For example, cubic ZrO_2 ($c\text{-ZrO}_2$) and fcc Ni has a larger lattice mismatch, which can be improved by increasing Pt content in $\text{Ni}_{1-x}\text{Pt}_x$ alloy.

The relaxed supercells were used to calculate the work function Φ of the metal alloys. By definition, the work function is calculated as the difference between the vacuum level (E_{vac}) and the Fermi energy (E_F) of the metal. The calculated work function Φ using different structure models, their average Φ_{av} , and the standard deviation s are summarized in Table I for various alloy compositions being considered. From these results, the following conclusions can be drawn. (i) For the same alloy composition, the work function Φ calculated using different structural models are very close (difference within 0.01 eV or 0.2%), which indicates that the distribution of Pt/Ni atoms or alloy disorder has little effect on the work function of the alloys. (ii) The work function decreases slowly with Pt content in the $\text{Ni}_{1-x}\text{Pt}_x$ alloy for a given surface composition, which implies that bulk alloy

TABLE I. The calculated work functions (Φ), their average (Φ_{av}), standard deviation (s), and formation energy of the (001) surface of $\text{Ni}_{1-x}\text{Pt}_x$ alloys.

x	Structure	Formation energy (eV/atom)	Φ (eV)	Φ_{av} (eV)	s (eV)
0.065	1a	-0.32	5.25	5.26	0.01
	1b	-0.32	5.25		
	1c	-0.29	5.26		
	1d	-0.28	5.27		
	1e	-0.28	5.25		
0.125	2a	-0.22	5.24	5.25	0.01
	2b	-0.21	5.25		
	2c	-0.20	5.24		
	2d	-0.18	5.26		
	2e	-0.22	5.24		
0.25	3a	-0.13	5.24	5.23	0.01
	3b	-0.14	5.24		
	3c	-0.13	5.23		
	3d	-0.13	5.23		
	3e	-0.14	5.22		
0.375	4a	-0.07	5.16	5.15	0.01
	4b	-0.05	5.14		
	4c	-0.06	5.15		
	4d	-0.06	5.16		
	4e	-0.07	5.16		

composition has a weak effect on the work function.

To compare the energetic and thermal stability of alloys with different compositions, we define and calculate their formation energies²⁴

$$E_{\text{form}} = [E_{\text{NiPt}} - E_{\text{Ni-slab}} + N_{\text{Pt}}(E_{\text{Ni-bulk}} - E_{\text{Pt-atom}})]/N_{\text{Pt}}, \quad (1)$$

where E_{NiPt} , $E_{\text{Ni-slab}}$, $E_{\text{Ni-bulk}}$, and $E_{\text{Pt-atom}}$ represent the DFT total energies of the NiPt surface, clean Ni(001) slab, bulk Ni (per atom), and isolated Pt atom, respectively; N_{Pt} is the

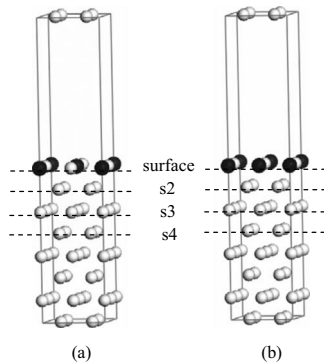


FIG. 4. Supercells of the $\text{Ni}_{1-x}\text{Pt}_x$ (001) surface. (a) Pt atoms along [110] direction. (b) Pt atoms along [100] direction. In the clean Ni surface, no Pt atoms is present. In the surface, s2, s3, and s4 models, the 50–50 mixed Pt and Ni layer is in the surface, the second, the third, and in the fourth layers, respectively (light: Ni; black: Pt).

number of Pt atoms in the supercell. Equation (1) should give a good estimate for the stability of the NiPt alloys with low Pt concentration. The calculated formation energies are also listed in Table I for various structures being considered. It can be seen that the differences in formation energies calculated using different structural models are small for a

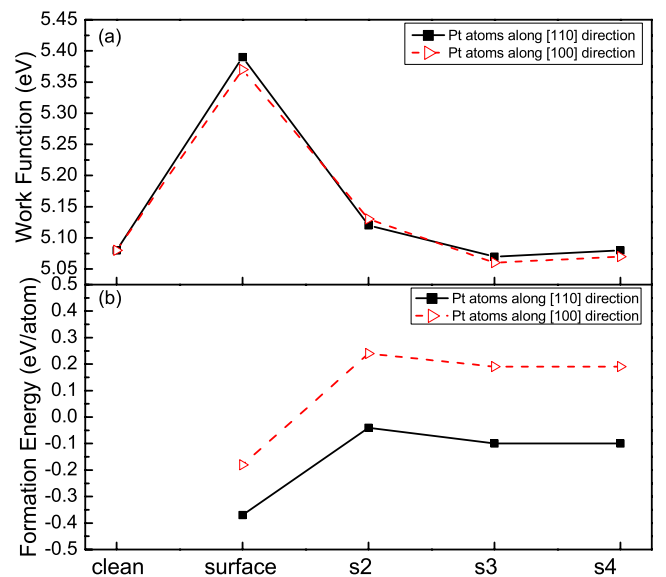


FIG. 5. (Color online) Work functions and formation energies of the five types of surface models: “clean,” “surface,” “s2,” “s3,” and “s4.”

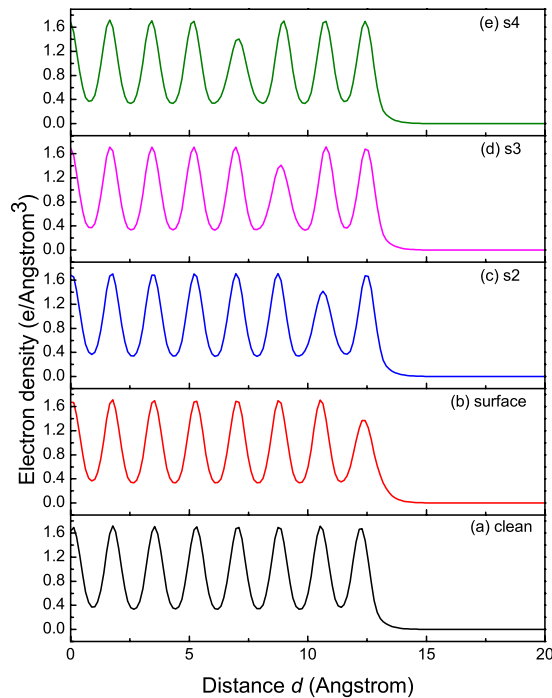


FIG. 6. (Color online) Plane-average electron charge density along the surface-normal direction for the five surface models: “clean,” “surface,” “s2,” “s3,” and “s4.”

given alloy composition. This is expected for alloys with low Pt concentration. Furthermore, the formation energy becomes less negative with increasing Pt content indicating that the alloy becomes less stable with increasing Pt doping.

B. Surface effects on work function

Next, we consider the effect of surface on the work function of the metal alloys. Here a supercell containing eight layers of a 2×2 surface unit cell is used. We further assume that only one of the eight layers is doped with Pt and all other layers contain only Ni atoms. The doped layer is assumed to contain equal amount of Pt and Ni atoms but they form two patterns with the Pt atoms forming rows along the [100] and [110] directions, respectively, as shown in Fig. 4. Furthermore, we compare the work functions of (1) a clean Ni surface (referred as a clean model in the following), and when the doped layer is (2) the top (surface) layer (surface model), (3) the second layer (s2), (4) the third layer (s3), and (5) the fourth layer (s4) of the Ni surface, respectively.

The calculated work functions and formation energies of the five models are shown in Figs. 5(a) and 5(b), respectively. Figure 5(a) shows clearly that Pt atoms in the surface layer increase significantly the metal work function. Second, the work functions calculated using the two patterns of Pt in the doped layer are almost identical. This indicates that the work function is insensitive to the distributions of Ni/Pt atoms for a given Pt doping content. This is consistent with the results obtained in bulk NiPt discussed in Sec. III A. However, the presence of Pt atoms in the surface layer has a significant effect on the work function of NiPt alloys. As seen in Fig. 5(a), replacing 50% of the Ni atoms by Pt atoms

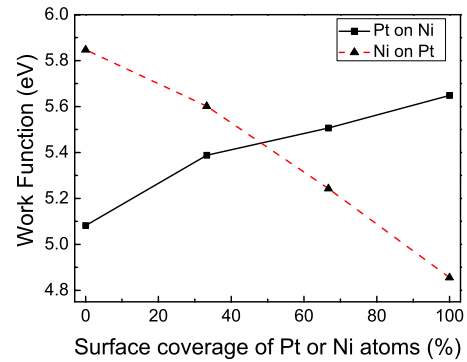


FIG. 7. (Color online) Variation of work function with Pt or Ni composition in the surface layer.

in the surface-layer results in an increase of about 0.32 eV or 6% in the work function compared to the work function of the clean Ni surface. When the mixed Pt and Ni layer is placed in the third (s3) or fourth (s4) layer, the work function is not much different from that of the clean Ni surface. It is also noted from Fig. 5(b) that the formation energy of the surface model is also energetically favored compared to other models.

Figures 6(a)–6(e) show the plane-averaged electronic charge density along the normal direction of the surface for the five surface models, respectively. Here, d is the distance in the surface-normal direction measured from the bottom layer of the slab. The figures demonstrate that while the charge density in the Pt-doped layer is smaller, its effect is only significant when it is the surface layer. The charge density near the surface and thus the metal work function is hardly affected by the Pt-doped layer when it is in the sub-surface layers. Results obtained here for the NiPt surface are consistent with those of nitrogen-doped molybdenum surface.²⁵ Electronic configurations of the Ni and Pt atoms are $3d^84s^2$ and $5d^96s^1$, respectively, indicating that the number of the valence electrons of Pt atom is smaller than that of Ni atom. Here, the valence electrons (shown by the integrated charge density) are mainly the s electrons. Therefore, when Ni atoms are substituted by Pt atoms, the total number of the covalent electrons in the doped layer is smaller than that of clean Ni layer. By this analysis, we can explain well the decrease of the plane-average electron charge density in the doped-Pt layer as seen in Figs. 6(a)–6(e).

We have carried out further calculations to investigate the dependence of work function on the composition of the surface layer. A similar supercell but with a larger (3×3) surface unit cell is used (Fig. 1). The supercell is also made up of eight layers of metal atoms. The different compositions in the surface layer are obtained by varying the ratio of the nine Pt and Ni atoms in the surface layer. For example, a 33.3% coverage of metal A on metal B means that there are three A atoms and six B atoms on both the top and bottom layers of the slab while the inner six metal layers consist of B atoms only. Figure 7 shows the variations of the calculated work functions with Pt and Ni compositions ($\text{Ni}_{1-x}\text{Pt}_x$ or $\text{Ni}_x\text{Pt}_{1-x}$) in the surface layer, respectively. It is clear that the surface doping has a significant effect on the metal work function. For example, the work function of $\text{Ni}_x\text{Pt}_{1-x}$ decreases by as

much as 1.0 eV when the surface Ni composition increases from zero up to one monolayer. Moreover, the work function changes gradually as the surface coverage increases. It is also noted that for the same surface composition with different inner metal layers, the work functions are different. For example, in terms of surface composition, 33.3% coverage of Pt on Ni is the same as 66.6% coverage of Ni on Pt. However, their work functions differ by 0.15 eV, which indicates that the substrate (inner layer) plays an important role in the work function.²⁶

IV. CONCLUSIONS

In conclusion, we have investigated the effects of disorder and surface-layer concentration on the work function of NiPt alloy as metal gate. It is found that for a given surface com-

position, disorder has little effect on the work function. However, surface-layer concentration has a significant effect on the work function. Moreover, our calculation predicts that Pt doping in the surface layer is energetically favorable. This work should provide experimentalists with some insights in their effort in atomic-level chemical modulation of work function of alloy metal gate.

ACKNOWLEDGMENTS

This work is supported by National Key Project for Basic Research of China under Grant No. 2005CB623605, Fund of National Engineering Research Center for Optoelectronic Crystalline Materials under Grant No. 2005DC105003, NSF of Fujian Province under Grant No. E0320002, and NSF of China under Grant No. 60876069.

*zghuang@fjnu.edu.cn

†phyfyp@nus.edu.sg

- ¹S. J. Wang and C. K. Ong, *Appl. Phys. Lett.* **80**, 2541 (2002).
- ²P. W. Peacock and J. Robertson, *Phys. Rev. Lett.* **92**, 057601 (2004).
- ³Y. F. Dong, Y. P. Feng, S. J. Wang, and A. C. H. Huan, *Phys. Rev. B* **72**, 045327 (2005).
- ⁴V. V. Afanas'ev, M. Houssa, A. Stesmans, and M. M. Heyns, *J. Appl. Phys.* **91**, 3079 (2002).
- ⁵Y. F. Dong, S. J. Wang, J. W. Chai, Y. P. Feng, and A. C. H. Huan, *Appl. Phys. Lett.* **86**, 132103 (2005).
- ⁶S. Park, L. Colombo, Y. Nishi, and K. Cho, *Appl. Phys. Lett.* **86**, 073118 (2005).
- ⁷H. N. Alshareef, K. Choi, H. C. Wen, H. Luan, H. Harris, Y. Senzaki, P. Majhi, B. H. Lee, R. Jammy, S. Aguirre-Tostado, B. E. Gnade, and R. M. Wallace, *Appl. Phys. Lett.* **88**, 072108 (2006).
- ⁸I. De, D. Johri, A. Srivastava, and C. M. Osburn, *Solid-State Electron.* **44**, 1077 (2000).
- ⁹Y. F. Dong, S. J. Wang, Y. P. Feng, and A. C. H. Huan, *Phys. Rev. B* **73**, 045302 (2006).
- ¹⁰C. Ren, D. S. H. Chan, X. P. Wang, B. B. Faizhal, M.-F. Li, Y.-C. Yeo, A. D. Trigg, A. Agarwal, N. Balasubramanian, J. S. Pan, P. C. Lim, A. C. H. Huan, and D.-L. Kwong, *Appl. Phys. Lett.* **87**, 073506 (2005).
- ¹¹V. Misra, G. P. Heuss, and H. Zhong, *Appl. Phys. Lett.* **78**, 4166 (2001).
- ¹²R. T. P. Lee, S. L. Liew, W. D. Wang, E. K. C. Chua, S. Y. Chow, M. Y. Lai, and D. Z. Chi, *Electrochem. Solid-State Lett.* **8**, G156

(2005).

- ¹³V. Misra, H. Zhong, and H. Lazar, *IEEE Electron Device Lett.* **23**, 354 (2002).
- ¹⁴R. Ishii, K. Matsumura, A. Sakai, and T. Sakata, *Appl. Surf. Sci.* **169-170**, 658 (2001).
- ¹⁵Bing-Yue Tsui, *IEEE Electron Device Lett.* **24**, 153 (2003).
- ¹⁶M. C. Payne, M. P. Teter, D. C. Allan, T. A. Arias, and J. D. Joannopoulos, *Rev. Mod. Phys.* **64**, 1045 (1992).
- ¹⁷G. Kresse and J. Furthmuller, *Comput. Mater. Sci.* **6**, 15 (1996).
- ¹⁸J. P. Perdew, J. A. Chevary, S. H. Vosko, K. A. Jackson, M. R. Pederson, D. J. Singh, and C. Fiolhais, *Phys. Rev. B* **46**, 6671 (1992).
- ¹⁹G. Kresse and D. Joubert, *Phys. Rev. B* **59**, 1758 (1999).
- ²⁰W. H. Press, B. P. Flannery, S. A. Teukolsky, and W. T. Vetterling, *New Numerical Recipes* (Cambridge University Press, New York, 1986).
- ²¹Paul C. Rusu and Geert Brocks, *Phys. Rev. B* **74**, 073414 (2006).
- ²²C. P. Herrero, L. Utrera, and R. Ramirez, *Phys. Rev. B* **46**, 787 (1992).
- ²³U. Kumar, K. G. Padmalekha, P. K. Mukhopadhyay, D. Paudyal, and A. Mookerjee, *J. Magn. Magn. Mater.* **292**, 234 (2005).
- ²⁴D. W. Yuan, X. G. Gong, and Ruqian Wu, *Phys. Rev. B* **75**, 233401 (2007).
- ²⁵A. M. Black-Schaffer and K. Cho, *J. Appl. Phys.* **100**, 124902 (2006).
- ²⁶Y. Jia, B. Wu, H. H. Weitering, and Z. Zhang, *Phys. Rev. B* **74**, 035433 (2006).